Published in final edited form as:
Am J Physiol Regul Integr Comp Physiol. 2008 January ; 294(1): R162–R171.

Endometriosis as a neurovascular condition: estrous variations in innervation, vascularization, and growth factor content of ectopic endometrial cysts in the rat

Guohua Zhang, **Natalia Dmitrieva**, **Yan Liu**, **Kristina A. McGinty**, and **Karen J. Berkley**
Program in Neuroscience, Florida State University, Tallahassee, Florida

Abstract

Endometriosis is a poorly understood, estradiol-dependent condition associated with severe pelvic pains and defined by vascularized endometrial growths outside the uterus. Endometriosis is produced in cycling rats by autotransplanting pieces of uterus onto abdominal arteries where they develop into cysts. The surgery induces vaginal and abdominal muscle hyperalgesia, whose severity is greatest in proestrus and nearly absent in estrus. The cysts contain growth factors and cytokines and develop their own sympathetic and sensory C- and Aδ-fiber innervation. Here, we used quantitative immunostaining and protein array analyses to test the hypothesis that the innervation and growth factor/cytokine content of the cysts, but not uterine horn, contribute to proestrous-to-estrous changes in hyperalgesic severity. If so, these characteristics in the cysts, but not the uterine horn, should change with estrous stage. In cysts, the density of sympathetic (but not sensory) neurites and amounts of NGF and VEGF proteins (but not cytokines IL-1, IL-6, IL-10, or TNF-α) were greater in proestrus than estrus. These changes were accompanied by vascular changes. Both sympathetic and sensory fibers in both stages colabeled with TrkA, indicating that changes in NGF could act on both afferent and efferent fibers. In contrast with the cysts, no changes occurred in the uterine horn between proestrus and estrus. Together, these results suggest that coordinated proestrous-to-estrous changes in innervation and vascularization of the cysts contribute to similar changes in hyperalgesic severity. The findings also encourage consideration of endometriosis as a neurovascular condition.

Keywords

angiogenesis; nerve sprouting; transplantation; inflammation; neurovascular coupling

Endometriosis (ENDO) is a condition in women of childbearing age defined by the presence of endometrial growths outside the uterus (ectopic growths). Its major symptoms include subfertility, severe dysmenorrhea (pain with menstruation), dyspareunia (vaginal hyperalgesia), dyschezia (pain with defecation), and chronic pelvic pain. ENDO often co-occurs with other painful disorders. It is considered dependent on estrogens because the growths and symptoms disappear with menopause. Consistent with this conclusion, the most successful and common treatment for ENDO's symptoms are hormonal agents that produce a hypoestrogenic state (28). Mechanisms underlying the pains of endometriosis are poorly understood (8).

ENDO is surgically induced in rats by autotransplanting on abdominal arteries small pieces of uterine horn that grow into vascularized cysts (67). Rats with surgically induced ENDO exhibit symptoms similar to those of women. Like women with ENDO, rats with ENDO are subfertile

Address for reprint requests and other correspondence: K. J. Berkley, Program in Neuroscience, Eppes Hall, 134 Convocation Way, Florida State Univ., Tallahassee, FL 32306-1270 (e-mail: kberkley@psy.fsu.edu).

(59). Once the cysts are fully developed, the rats also develop a vaginal hyperalgesia (15) that is accompanied by referred abdominal muscle hyperalgesia (46). In support of the clinical conclusion that ENDO is dependent on estrogens, the severity of both the vaginal and referred abdominal muscle hyperalgesia in rats varies with estrous stage in a manner that parallels estrous changes in circulating levels of estradiol. Specifically, the severity is greatest in proestrus when estradiol levels are high and lowest in estrus when estradiol levels fall to nearly zero (6).

The cysts in rats and women share many structural and molecular features (58). The growths contain or evoke abnormal production in nearby tissues of many substances that have been hypothesized to play as yet unspecified roles in the signs and symptoms of ENDO. These substances include, among others, cytokines such as IL-1, IL-6, IL-8, and IL-10, TNF-α, and growth factors, such as VEGF and NGF (3,12,27,32).

Recently, it has also been shown that the cysts in rats and women develop their own sensory and sympathetic innervation (7,8). The fibers appear to sprout from paravascular and perivascular nerve fibers that accompany the blood vessels as they vascularize the growths (7). It seems likely that this innervation, particularly the sensory innervation, and the cysts' contents of cytokines, especially pro-inflammatory cytokines, and growth factors, contribute to the severity of ENDO's symptoms, in particular, their variation with estrous stage. Accordingly, here, we tested this hypothesis by quantitative comparison of the innervation, cytokines, and growth factors in fully grown cysts harvested from rats in proestrus and estrus. Furthermore, if indeed it is the cysts that contribute to the vaginal hyperalgesia, then such changes should not necessarily be expected to occur in the healthy uterus. Therefore, we also assessed changes in these characteristics in proestrus and estrus in the healthy uterus from the same rats.

Methods

Subjects

Adult female Sprague-Dawley rats (Charles River, Wilmington, MA; Raleigh, NC, facility) were used (n = 20). They were housed individually, with ad libitum access to rat chow and water, and maintained under controlled conditions (24°C, 12:12-h light-dark cycle with lights on at 7:00 AM). Estrous stage was monitored daily by vaginal lavage ~2 h after lights on, beginning at least 2 wk before surgery and continuing until the day of death. The traditional method of estrous nomenclature was followed (see figure 3 in Ref. 6). Only rats with regular 4-day cycles, both before and after surgery, were used. Rats weighed ~225 g at the time of the ENDO surgery and ~300 g when the cysts were harvested. All experiments were performed in accordance with the National Institutes of Health Guide for the Care and Use of Laboratory Animals (NIH Publications No. 86–23), revised in 1985. Efforts were made to minimize both the animal's suffering and the number of rats used. The study was approved by Florida State University's Institutional Animal Care and Use Committee as protocol no. 9028.

Experimental Strategy

The study was done in two parts in two separate groups of rats. In both groups, surgical induction of endometriosis by autotransplantation of four pieces of uterine horn (taken from the middle of the left uterine horn) onto abdominal arteries was performed. Most of these autotransplants form round or oval-shaped cysts that gradually increase in size over a period of ~8–10 wk before stabilizing in size (67). Accordingly, for both groups, ~11 wk after surgery, rats in either proestrus or estrus were anesthetized with urethane (1.2 g/kg ip). Each transplant region was identified (by the suture), and those transplants that had formed cysts were carefully dissected from their surrounding tissue, and their largest and smallest diameters were measured.

In addition, a 1-cm length of the middle of the healthy right uterine horn was identified; i.e., the same area that had been taken from left uterine horn and used for the transplants. Importantly, there were no proestrous-estrous differences either in the proportion of the four implants that had formed cysts, which ranged from 2 to 4 per rat, or in cyst size ($P > 0.05$).

In one group ($n = 8$), the rats were perfused transcardially with saline followed by 4% paraformaldehyde in 0.1 M phosphate buffer (PB, pH 7.4). Next, the previously measured cysts and the previously identified pieces of right healthy uterine horn were harvested and processed for immunostaining with markers specific for different neurites, which could then be quantified. In the other group ($n = 12$), all cysts and pieces of healthy uterine horn were immediately harvested and prepared for quantitative analyses of their contents of cytokines and growth factors using protein antibody arrays. Please note that throughout this paper, the word “marker” and phrase “neurite density” are used to refer to results from the immunostaining study, whereas the word “antibody” and the phrase “spot density” are used to refer to results from the protein array study.

Surgical Induction of ENDO

Surgery was done following aseptic precautions. Rats in estrus were anesthetized with a mixture of ketamine hydrochloride and xylazine (73 and 8.8 mg/kg ip, respectively). A midline abdominal incision exposed the uterus, and a 1-cm segment of the middle of the left uterine horn was removed and placed in warm sterile saline. Four pieces of uterine horn (~2 × 2 mm) were cut from this segment and sewn, using 4.0 nylon sutures, around alternate cascade mesenteric arteries that supply the small intestine, starting from the cecum. The incision was closed in layers, and the rat was allowed to recover from anesthesia. Postoperative recovery was uneventful, and regular estrous cyclicity resumed in all rats within ~1 wk.

Immunohistochemistry

For single labeling, sections were immunostained by one of the following three markers: the sympathetic fiber marker, vesicular monoamine transporter 2 (VMAT2; 69), and the C- and Aδ- sensory fiber markers, CGRP (48), and transient receptor potential vanilloid-1 (TRPV1; 48). For double labeling, sections were immunostained with the high-affinity receptor for NGF, tyrosine kinase A (TrkA), and VMAT2, or CGRP.

The cysts and pieces of uterine horn were harvested as described in *Experimental strategy*. In total, there were sections through nine cysts and four pieces of uterine horn from four rats in proestrus, and twelve cysts and four pieces of uterine horn from four rats in estrus. Upon removal, the samples were postfixed in the same fixative solution for 4 h, and then cryoprotected in 30% sucrose in 0.1 M PB for 48 h at 4°C. Twenty-micrometer-thick transverse sections were cut serially, using a cryostat, through each cyst or uterine horn and thaw-mounted at 160-μm intervals (i.e., on sets of 8 slides). Slides were stored in a −20°C freezer until immunostaining.

Sections were quenched with 0.3% H_2O_2 for 10 min and then blocked in 0.3% Triton X-100 in 0.05 M Tris-NaCl with 10% normal goat serum (NGS) for 1 h. Thereafter, sections were incubated with rabbit anti-VMAT2 (1:15,000; Chemicon, Temecula, CA), or rabbit anti-CGRP (1:15,000; Chemicon), or guinea pig anti-TRPV1 (1:10,000; Neuromics, Minneapolis, MN) in 0.3% Triton X-100 in 0.05 M Tris-NaCl, including 2% NGS at 4°C overnight. The next day, sections were incubated in biotinylated goat anti-rabbit (or anti-guinea pig accordingly) IgG (1:300; Vector Laboratories, Burlingame, CA) at room temperature (RT) for 2 h followed by incubation in avidinbiotin-peroxidase complex (Elite kit, Vector Laboratories) for 1.5 h. Staining was visualized with 3,3′-diaminobenzidine (DAB kit, Vector Laboratories). For each marker, the dilution used was the one that in the test sections produced maximal labeling of

neurites with minimal background. Slides containing sections of all samples were processed together so that the staining would be as consistent as possible. Controls for all markers included omission of the primary antibody, omission of the secondary antibody, and absorption of the primary antiserum with its respective antigen prior to use. There was no labeling in any of the control sections.

After being blocked in 0.05 M phosphate-buffered saline with 10% normal donkey serum, sections from 6 cysts from rats in proestrus and 5 cysts from rats in estrus were incubated with a mixture of rabbit anti-VMAT2 (1:1,000; Chemicon, Temecula, CA) and goat anti-TrkA (1:1,500; R&D Systems, Minneapolis, MN), or a mixture of rabbit anti-CGRP (1:3,000; Chemicon) and goat anti-TrkA (1:1,500; R&D Systems) at 4°C overnight. The next day, after being rinsed, sections were incubated with a mixture of Cy2-conjugated donkey anti-rabbit IgG (1:300; Jackson ImmunoResearch, West Grove, PA) and Rhodamine Red-X-conjugated donkey anti-goat IgG (1:300; Jackson ImmunoResearch) at RT for 1 h. Sections were then rinsed and mounted with Gel/Mount fluorescence mounting medium (Abcam, Cambridge, MA).

Every attempt was made to ensure that counts of neurites in the sections of the cysts and uterine horn in proestrus and estrus were done consistently. First, one of the sections that was in the middle of the cyst (had the largest diameter) and that had the densest population of neurites was chosen. The section usually included the hilus region, which is the area where blood vessels are clearly seen to enter the cyst and which has the densest population of neurites, outlined in Fig. 2, A and B). Likewise, a section from the middle of the set of sections of the uterine horn was chosen to include the area where the uterine artery enters (outlined in Fig. 3, A and B). These cyst and uterine horn sections were identified on each of the sets of slides that had been immunostained using a different marker antibody. Thus, the chosen sections that had been immunostained with different markers were adjacent to each other. Next, each of the chosen sections was photographed with an Optronics Microfire camera (Optronics International, Chelmsford, MA) and Neurolucida software (MBF Laboratories, Williston, VT). The images were then exported in coded form to a computer for quantification using the Stereo Investigator program.

On each section, using the program, one experimenter outlined the hilus region on the section where innervation was densest or a similar region on sections of the uterine horn (shown in Figs. 2, A and B and 3, A and B). The outline was entered into the program, which calculated the area of that outlined region in square millimeters. The area of the regions did not differ by estrous stage ($P > 0.05$). After selecting the region in which neurites were to be counted, each neurite within this area was marked by two investigators blinded to estrous stage. Neurites were identified as thin, relatively straight black lines, distinct from the background, sometimes beaded with varying width, and sometimes branched. Each straight continuous or beaded line was counted as one neurite, while the tip of each branch was counted as another neurite. The numbers of neurites labeled by VMAT2, CGRP, or TRPV1 within each outlined region and the measurements of the area of each region were exported to spreadsheets for calculation of the number of neurites/mm^2 and statistical analyses. Counts by the two investigators were highly correlated ($r > 0.85$ for all counts). Calculations were therefore done using averages of the two sets of counts.

Protein Arrays

The cysts and pieces of uterine horn were harvested as described in *Experimental strategy*. In total, 15 cysts and 6 pieces of uterine horn from 6 rats in proestrus, and 11 cysts and 6 pieces of uterine horn from 6 rats in estrus were harvested. Once harvested, they were immediately cut into small pieces in cold microcentrifuge tubes, and then sonicated in cold lysis buffer (25 mM HEPES, 1 mM EDTA, 6 mM $MgCl_2$, 1 mM DTT, 1 μg/ml proteinase inhibitors, pH 7.4).

The extraction solution was centrifuged at 14,000 rpm at 4°C for 30 min. The supernatant was aliquoted and stored at −80°C until use. The total protein concentration of each sample was determined by BCA protein assay kit (Pierce, Rockford, IL).

Protein array membranes (Rat Cytokine Antibody Array Kit, RayBiotech, Norcross, GA), were processed using the kits supplied according to the manufacturer's instructions. Each “Rat Cytokine Array” membrane from RayBiotech contains double “spots” of antibodies for 19 different growth factors and cytokine antibodies. Each membrane also contains double positive and negative control spots. The antibodies for each protein had been validated by RayBiotech as specified on their website http://www.raybiotech.com/cytokine_antibody_array.asp).

Each membrane was blocked in 2 ml blocking buffer for 1 h. Next, 500 μg (100–200 μl) of total protein from a single cyst was loaded onto the membrane, and the reaction volume was adjusted to 1.0 ml by adding the appropriate amount of blocking buffer, and incubated at 4°C overnight. After several washes, each membrane was incubated in biotin-conjugated antibody for 2 h followed by HRP-conjugated streptavidin for 1 h. Each membrane was treated with a chemiluminescent solution and exposed to X-ray film. The film was then developed.

To ensure that processing conditions were as identical as possible for all samples, 500 μg of protein from samples of cysts or uterine horn in proestrus and estrus were loaded on different membranes and processed simultaneously in large groups. This strategy permitted valid comparisons of relative differences in concentration between samples from different groups for each of the antibodies on the array.

The signal intensity of individual “spots” on the developed X-ray film for each sample was measured using the NIH ImageJ program (http://rsb.info.nih.gov/ij/). The spots measured were of antibodies for VEGF, NGF, IL-1β, IL-6, IL-10, and TNF-α, as well as the negative and positive control spots. The *inset* in Fig. 5A shows examples from films of processed double spots for VEGF and positive and negative controls, one in proestrus, the other in estrus.

To measure the signal intensity of each spot, the experimenter, blinded to estrous stage and tissue, placed a standard-sized circle over each spot. The program then measured the signal intensity of labeling of that outlined spot on the film. Signal intensities of the two spots for each cytokine and growth factor and the controls were averaged. To control for differences between membranes, the signal intensities of VEGF, NGF, IL-1β, IL-6, IL-10, and TNF-α on each film were normalized against both positive and negative controls. The data were then exported to spreadsheets for statistical analyses.

Vascular Characteristics

Photomicrographs of an entire cross section through the middle of each cyst (six each from proestrus and estrus, selected at random from the full set) and uterine horn (four each) were imported in coded form into Stereo Investigator. An investigator examined each section at low power and entered outlines of the outer and inner (lumen) contours of that sample into the Stereo Investigator program, which then calculated the lumen area and the total outer area. Calculation of the actual area being assessed (i.e., the “wall” of the cyst or uterus sample) was done by subtracting the lumen area from the outer area.

Next, at higher power, using consistent criteria for all samples, the same investigator systematically scanned the entire cyst or uterine wall and entered an outline of the contour of each visible blood vessel in the section into the program, which automatically calculated the area of that blood vessel. The investigator also drew a line across the shortest diameter of each blood vessel. Blood vessels appeared as rounded or oval openings lined by endothelial cells. Examples of such blood vessels can be seen in Fig. 1B.

The following data were entered from the Stereo Investigator program into spreadsheets for each cyst or uterine sample: *1*) total area of the cyst or uterine section; *2*) area of the lumen of the cyst or uterus; *3*) areas of each of the blood vessels in that sample; and *4*) diameter of each blood vessel. These four data sets allowed calculation for each sample of *1*) area of the "wall" of that sample; *2*) the percent area occupied by blood vessels in that sample; *3*) the number of blood vessels in that sample; and *4*) the mean diameter of the blood vessels in that sample. The codes were then broken so that comparisons could be made between cysts and uterine horn samples from rats in proestrus vs. estrus. Note that, for samples of uterine horn and cysts, the areas of their walls did not differ by estrous stage ($P > 0.05$, unpaired *t*-test).

Data Analysis

Using Statistical Package for the Social Sciences ver. 13 software (SPSS, Chicago, IL), differences between groups were initially assessed with two-way ANOVAs, followed, if significant, by one-way ANOVAs, which, in turn, if significant, were followed by post hoc Tukey tests. In addition, independent *t*-tests were used to assess significance of estrous differences in the overall size of the cysts, the areas of the "hilus" region of cysts and uterine horn, and the areas of the whole sections of cysts and uterine horn. Significance was set at $P \leq 0.05$.

Results

The distribution patterns of positively stained neurites in the fully grown cysts were virtually identical to those described previously (7). Briefly, the cysts were robustly innervated, with the densest innervation at the hilus region progressively lessening further away from the hilus. Both sympathetic (VMAT2-positive) and sensory fibers (CGRP-positive and TRPV1-positive) accompanied blood vessels as they entered the cyst at the hilus and through the cyst wall, with small bundles and individual fibers extending into the myometrium and eventually into the endometrial stroma and the epithelium lining the lumen. Figure 1 provides an example of VMAT2-positive immunostaining of neurites mainly around blood vessels at the hilus entrance (Fig. 1, A and B, arrows) and, further into the cyst wall, of neuritis mainly in the endometrial stroma. A similar pattern existed for the uterine horn.

Sympathetic, but not Sensory, Innervation of the Cysts is Greater in Proestrus Than Estrus

Because neurite labeling with all markers was densest in the hilus area of the cyst, and the average size of the cysts did not differ in proestrus and estrus ($P > 0.05$), quantitative analyses of the labeling were carried out in approximately the same region in the hilus area in all cysts (outlined in Fig. 2, A and B). Two-way ANOVAs indicated that the density of neurites in this region varied significantly by marker [$F(2,50) = 3.77$, $P < 0.05$], with a significant stage by marker interaction [$F(2,50) = 3.76$, $P < 0.05$]. Thus, overall, the density of neurites was significantly influenced by estrous stage.

When comparing between estrous stages using one-way ANOVAs followed by post hoc Tukey tests, the density of sympathetic neurites stained by VMAT2 was significantly greater in proestrus than in estrus ($P < 0.05$). Surprisingly, however, the number of sensory neurites stained by CGRP or TRPV1 showed no significant estrous differences. These effects can be seen qualitatively by comparing the left and right columns of photomicrographs in Fig. 2, and quantitatively by the graphs in Fig. 4A.

Within each stage, one-way ANOVAs indicated that, overall, there were only a few differences in neurite density between the different markers (Fig. 4A). Thus, in proestrus, the density of VMAT2-positive neurites was significantly greater than TRPV1-positive neurites, whereas, in estrus, there were no significant differences between the densities of the different markers.

No Estrous Differences in Uterine Horn Innervation

To compare labeling in the uterine horn with that in the cysts, a region as comparable as possible to the hilus of the cyst was assessed. This region is located where the ovarian artery enters the uterine horn (outlined in Fig. 3, A and B; compare with the outlined regions in Fig. 2, A and B). The distribution patterns of positively stained neurites in this region were similar to those in the cysts, and comparable to those reported by others in the uterine horn (47, 49, 72). Furthermore, the density of neurites labeled with each of the three markers in the uterine horn did not differ significantly from the density of neurites labeled with each of the three markers in the cysts, regardless of estrous stage.

Although the density of neurites in the uterine horn, like that in the cysts, varied significantly by marker [$F(2,14) = 5.96$, $P < 0.02$], there were few differences between the markers (Fig. 4B). The only difference was that there were fewer TRPV1-positive neurites than VMAT2 and CGRP neurites ($P < 0.05$). Unlike the cyst, however, there was no significant stage by marker interaction [$F(2,14) = 0.04$, $P = 0.96$]. Thus, the density of neurites stained by each marker was not influenced by estrous stage. Although the graph in Fig. 4B suggests that the density of positively labeled neurites was, for each marker, consistently greater in proestrus than estrus, this apparent overall difference was not significant.

Protein Levels of Growth Factors VEGF and NGF, but not Cytokines IL-1-β, IL-6, IL-10, and TNF-α, Are Greater in Proestrus Than Estrus in Cysts; No Estrous Differences in Uterine Horn

To determine whether the contents of growth factors and cytokines in the cysts and uterine horn differed in proestrus and estrus, the fully grown cysts were analyzed quantitatively using measurements of normalized spot signal intensities for each antibody on films of the protein arrays. Although these analyses do not provide “absolute” values of the amount of each protein in the cysts or uterus, they do allow comparisons of “relative” changes between proestrus and estrus and between cyst and uterine samples because, as described in *Protein arrays*, processing and assessments of the membranes were performed in as identical a manner as possible.

Statistical analyses showed that the spot signal intensities differed significantly by estrous stage [$F(1,65) = 4.03$, $P < 0.05$], by tissue [$F(1,195) = 5.45$, $P = 0.02$], and by antibody [$F(5,195) = 9.99$, $P < 0.01$], with significant interactions between antibody and tissue [$F(5,195) = 8.76$, $P < 0.01$] and between antibody and estrous stage [$F(5,195) = 2.42$, $P < 0.05$]. Thus, the spot signal intensity for each antibody on the film was influenced by both the tissue (cyst vs. uterine horn) and the stage in which it was taken (proestrus vs. estrus). These differences are illustrated in Fig. 5, A and B. Comparisons between the cysts and uterus of the spot signal intensity for each marker showed that the only marker in which differences between the cysts and uterine horn was found was VEGF in proestrus ($P = 0.007$). Thus, in proestrus, but not in estrus, there was more VEGF in the cysts than in the uterus.

In the cysts (Fig. 5A), there were significant differences in spot signal intensity by antibody [$F(5,136) = 21.64$, $P < 0.01$] and by stage [$F(1,136) = 9.59$, $P < 0.01$], with a significant interaction between them [$F(5,136) = 5.39$, $P < 0.01$]. Thus, for the cysts, spot signal intensities of the antibodies were significantly influenced by the stage in which they were measured.

In proestrus (Fig. 5A, solid bars), spot signal intensities of the VEGF antibody were greater than those for all other antibodies, and spot signal intensities for the NGF antibody were greater than those for all other antibodies except TNF-α. Spot signal intensities for ILβ, IL-6, IL-10, and TNF-α did not differ significantly from each other.

In estrus (Fig. 5A, open bars), the spot signal intensity for the VEGF antibody was significantly more intense than the spot signal intensity for IL-1β, IL-6, IL-10, but not for the spot signal intensities of the NGF and TNF-α antibodies.

In other words, spot signal intensities for the two growth factor antibodies, VEGF and NGF, were generally greater than spot signal intensities for the cytokine antibodies, IL1β, IL-6, IL-10, and TNF-α, and these differences were more prominent in proestrus than in estrus. These differences resulted in there being a significant difference between proestrus and estrus in the spot signal intensities of the VEGF and NGF antibodies. In other words, in the cysts, there was more VEGF and NGF in proestrus than in estrus and no estrous differences in the cysts' contents of cytokines.

In the uterine horn (Fig. 5B), in contrast to the cysts, although there was a significant difference in the spot signal intensities of the different antibodies [$F(1,59) = 2.70$, $P = 0.03$], there were no differences by stage [$F(1,59) = 0.028$, $P = 0.87$], nor was there an interaction of antibody with stage [$F(5,59) = 0.10$, $P = 0.99$]. Furthermore, post hoc Tukey tests revealed no significant differences in the spot signal intensities of the different antibodies in either proestrus or estrus.

Cysts Were Less Vascularized in Proestrus Compared with Estrus, But There Were no Changes Between These Two Stages in Vascularization of the Uterine Horn

The dramatic proestrous to estrous changes in VEGF antibody staining in the cysts but not the uterus led us to consider whether these changes were accompanied by comparable changes in the vascularization of the two tissues. We did this assessment by quantifying, in the entire cyst and uterine horn, the percentage of the total area occupied by blood vessels, their diameter, and how many of them there were in the cysts and uterine horn in proestrus and estrus. Again, like assessments of spot densities, although absolute values of vascularization are not meaningful, relative changes in vascularization between proestrus and estrus and between the cyst and uterine samples are meaningful, because, as described in *Protein arrays*, every effort was made to make the assessments comparable. The results are shown in Fig. 6.

We found, using two-way ANOVAs (comparing by tissue and estrous stage), that although the percentage of the *total area* occupied by blood vessels in the cysts and uterus did not differ from each other [$F(1,18) = 1.48$, $P = 0.24$], the percentage of the total area occupied by blood vessels did differ by estrous stage [$F(1,18) = 9.47$, $P < 0.01$]. Similarly, the diameter of blood vessels in the cysts and the uterus did not differ from each other [$F(1,18) = 0.01$, $P = 0.92$]. Although the diameters did not vary with estrous stage [$F(1,18) = 0.66$, $P = 0.43$], there was a significant interaction between tissue and estrous stage [$F(1,18) = 4.74$, $P = 0.04$]. The biggest effects were in the “number of blood vessels” in the cysts and uterus, which differed significantly by tissue [$F(1,18) = 4.68$, $P = 0.04$] and by estrous stage [$F(1,18) = 12.26$, $P = 0.01$], with a significant interaction between them [$F(1,18) = 8.40$, $P = 0.01$].

Taken together, what these analyses mean is that, in the cysts (Fig. 6, A, C, and E), from proestrus to estrus, there was an insignificant decrease in the diameter of blood vessels (Fig. 6E) and a large, significant increase in their number (Fig. 6C). Together, these changes resulted in an overall significantly greater percentage in estrus compared with proestrus of the total area of the cyst wall that was occupied by blood vessels (Fig. 6A). In contrast, for the uterine horn (Fig. 6, B, D, and F), although the percentage of the total area occupied by blood vessels when collapsed across the two estrous stages did not differ from that of the cysts, there were no significant proestrous-to-estrous changes in any vascular measure.

Markers for the NGF Receptor, TrkA, Colocalize With Markers for Both Sensory (CGRP) and Sympathetic (VMAT2) Fibers in the Cysts

NGF influences the functions of both sensory and sympathetic fibers (62). Therefore, the estrous changes in NGF levels in the cysts that were observed here could exert influences on either type of fiber. It was therefore of interest to determine whether the protein receptor for NGF, i.e., TrkA, was located on sensory or sympathetic fibers in the cysts. Accordingly, we

carried out double-labeling immunostaining with TrkA and CGRP or TrkA and VMAT2. In both proestrus and estrus, we found that in the region of the hilus ~30% of the TrkA-positive neurites were double-labeled with CGRP or with VMAT2 (Fig. 7).

Discussion

Our initial hypothesis was that proestrous-to-estrous changes in sensory innervation and cytokine content of the cysts, but not the uterine horn, contribute to proestrous-to-estrous differences in severity of ENDO-induced hyperalgesia (15,46). We did observe estrous changes in the cysts but not the uterine horn. However, it was the density of sympathetic, not sensory fibers, in the cysts and their contents of growth factors VEGF and NGF, not cytokines IL-1, IL-6, IL-10, and TNF-α, that changed. These changes were accompanied by changes in vascularization of cysts but not the uterine horn. Although our findings would appear to indicate that only efferent fibers and vascularization changed between proestrus and estrus, the fact that the NGF receptor protein, TrkA, was localized on both sensory and sympathetic fibers, suggests that activities of both afferent and efferent fibers in the cysts might change and therefore that both types of fibers could contribute to the proestrous-to-estrous changes in hyperalgesic severity.

Sympathetic Involvement in ENDO-Induced Hyperalgesia

There is considerable support for involvement of peripheral sympathetic (as well as sensory) fibers in hyperalgesia. Numerous studies have shown that peripheral nerve injury generates sympathetic sprouting surrounding primary afferent neurons and fibers in the periphery (29, 57,71), as well as in dorsal root ganglia (17,41,52). It is thought that this reorganization leads to chemical coupling between sympathetic and afferent neurons that sensitizes and/or activates primary afferent nociceptors. One likely mediator is norepinephrine (2,16,20), but it is unknown which adrenoceptor subtype is involved because their expression and effects vary with pathophysiological condition (9), time following injury (43), and strain (4). If such effects pertain here, it remains to be determined what adrenoceptor subtypes are involved.

Multiple Potential Roles for NGF/TrkA Signaling in Endometriosis Via Sensory and Sympathetic Fibers

It is well known that NGF levels increase in inflamed tissues, which can lead to hyperalgesia by both peripheral and central mechanisms (50). Peripherally, NGF directly activates and sensitizes primary afferent nociceptors (56). Our results demonstrate the presence of TrkA on CGRP-positive sensory fibers, which are likely to be C- or Aδ-fiber nociceptors (33). Together, with the increase in NGF in the cysts during proestrus when hyperalgesia severity is greatest, these findings suggest that NGF directly activates C-fibers in cysts, thereby contributing to ENDO-induced hyperalgesia. This conclusion is consistent with clinical results showing that pain severity correlates with NGF levels in diseased tissues or extracellular fluid in conditions such as chronic prostatitis (44), interstitial cystitis (39), painful intervertebral disc (25), and finally, endometriosis (3).

Intriguingly, the facts that TrkA was localized on sympathetic fibers in cysts and that both NGF and the density of sympathetic fibers increased in proestrus in cysts suggests that, in addition to nociception, NGF induces sprouting of sympathetic fibers in cysts. This conclusion accords with other findings showing that neurotrophin growth factors and receptors are important regulators of development and maintenance of the nervous system, particularly NGF/TrkA signaling (37), and that NGF is involved in sympathetic sprouting, for example, after peripheral nerve injury (19,36). It is uncertain what produces increases in cyst NGF during proestrus. Consistent with the clinical conclusion that ENDO is an estrogen-dependent disorder (28), one likely contributor is estradiol, whose plasma levels gradually increase during the estrous cycle,

reaching their peak in proestrus (6). In support of this are studies demonstrating that estradiol stimulates expression of NGF and its receptors in uterine tissue, although effects of progesterone may also contribute (60). However, this conclusion raises the question of why increased levels of NGF were not observed in the uterine horn. One possibility is that the protein array method used here was not sensitive enough, which, if so, suggests that estradiol's putative influence on NGF levels in the cysts was greater than in uterine horn, possibly because of estradiol's actions on mast cells (10), which are more abundant in cysts and their luminal contents than in uterine horn.

Cytokine Involvement in ENDO-Induced Hyperalgesia

Proinflammatory cytokines such as IL-1β, IL-6, and TNF-α and the anti-inflammatory cytokine, IL-10, are strongly associated with a variety of hyperalgesic and pathological pain states (18,68,70). Unsurprisingly, therefore, elevated levels of these cytokines are observed in peritoneal fluid of women with endometriosis, suggesting their involvement in endometriosis and its symptoms (51,65). Thus, our finding that levels of these cytokines were the same in cysts and uterine horn and did not change from proestrus to estrus was surprising. This situation appears to suggest that cytokines may not be as important contributors to ENDO-induced hyperalgesia as are the growth factors discussed above. However, it is important to note that our extraction method used the entire cyst, which may not be suitable for assessment of the role of cytokines for two reasons. First, potential estrous changes in the cyst's luminal fluid may be obscured by a lack of such changes in the wall of the cyst. Second, cytokine contributions may be exerted via their release into peritoneal fluid, which was not measured here. Therefore, mechanisms of involvement of these cytokines in ENDO-induced hyperalgesia require further study.

VEGF Involvement in ENDO-Induced Hyperalgesia?

VEGF is a key regulator of angiogenesis (23), which is thought to be involved in the pathogenesis of endometriosis (30). Studies on women with endometriosis compared with healthy controls show differences in both peritoneal fluid composition and the eutopic and ectopic endometrium that relate to angiogenesis regulation (24,26,42). High VEGF concentrations are found in peritoneal fluid in pelvic endometriosis and in cystic fluid in ovarian endometriomata (22). Furthermore, in animal models, anti-VEGF compounds inhibit ectopic endometrial growth (5,34).

Interestingly, studies by some investigators suggest that angiogenesis in women with endometriosis may be related to pelvic pain (1,66). Our findings here that levels of VEGF were higher in proestrus compared with estrus in the cysts, but not uterine horn, support this idea to some extent. Of importance, however, is our finding that the total area occupied by blood vessels in the cysts increases the day after proestrus (i.e., in estrus), due mainly to an increased number of smaller-diameter vessels in estrus (i.e., likely newly sprouted vessels; Ref. 13). This finding is compatible with the fact that others have observed sex-steroid regulation of VEGF's role in the development of new blood vessels (35,45,61). Furthermore, the fact that we did not observe changes in VEGF or vascularization in the uterine horn is consistent with previous observations that no new vessel growth occurs during the estrous cycle in the rat uterus (54). These findings suggest that angiogenesis associated with increased levels of VEGF in proestrus in the cysts results in increased vascularization and remodeling of blood vessels that become evident the next day in estrus. It is therefore possible that VEGF's potential involvement in ENDO-induced hyperalgesia relates to potential associations between the initiation of sprouting of new blood vessels (i.e., angiogenesis) and the sprouting of new axons in the cysts (63).

Coordinated Innervation and Vascularization of the Cysts

Important clues concerning how the fully grown cysts develop their nerve supply are that their innervation is densest adjacent to blood vessels in the hilus and that neurites follow blood vessel walls, extending from them into myometrial and epithelial layers (7,8). This situation suggests that the developing innervation occurs via sprouting of perivascular and paravascular fibers accompanying the sprouting blood vessels that vascularize the cysts.

Perspectives and Significance

The results of this study fit contextually within the realms of both the vascular system and the nervous system. Although these systems seem to be functionally and structurally different, blood vessels and axons follow parallel routes in the periphery, with a two-way interaction between them (14,64). Furthermore, NGF can exert effects on endothelial cells as well as neurons, and VEGF can exert effects on neurons as well as blood vessels (38). It has therefore been suggested that these (and other) growth factors cooperate to coordinate reinnervation and vascularization not only of organ transplants (40,53,55) but also in diseases such as cancers that involve new tissue growth (38). Our findings showing dynamic estrous changes in both VEGF and NGF in the cysts, but not the uterine horn, in parallel with changes in the cysts' innervation and vascularization, suggest that this cooperative situation might apply to endometriosis as well. If so, it might be appropriate to consider endometriosis not only as a neuropathic condition (21), but also, like migraine headache (11,31), as a neurovascular disease. Such a change encourages future studies in both animal models and women on issues such as *1*) how factors involved in the coordinated modulation of vascular and neural physiology contribute to endometriosis and its pains, and *2*) potential common factors underlying migraine and endometriosis.

Acknowledgements

We thank Stacy McAllister for technical help and John Chalcraft for help with illustrations.

Grants

This study was supported by National Institutes of Health Grant RO1 NS11982.

References

1. Alcazar JL, Garcia-Manero M. Ovarian endometrioma vascularization in women with pelvic pain. Fertil Steril 2007;87:1271–1276. [PubMed: 17336965]
2. Ali Z, Raja SN, Wesselmann U, Fuchs PN, Meyer RA, Campbell JN. Intradermal injection of norepinephrine evokes pain in patients with sympathetically maintained pain. Pain 2000;88:161–168. [PubMed: 11050371]
3. Anaf V, Simon P, El N I, Fayt I, Simonart T, Buxant F, Noel JC. Hyperalgesia, nerve infiltration and nerve growth factor expression in deep adenomyotic nodules, peritoneal and ovarian endometriosis. Hum Reprod 2002;17:1895–1900. [PubMed: 12093857]
4. Banik RK, Sato J, Yajima H, Mizumura K. Differences between the Lewis and Sprague-Dawley rats in chronic inflammation induced norepinephrine sensitivity of cutaneous C-fiber nociceptors. Neurosci Lett 2001;299:21–24. [PubMed: 11166928]
5. Becker CM, Sampson DA, Rupnick MA, Rohan RM, Efstathiou JA, Short SM, Taylor GA, Folkman J, D'Amato RJ. Endostatin inhibits the growth of endometriotic lesions but does not affect fertility. Fertil Steril 2005;84:1144–1155. [PubMed: 16210006]
6. Becker JB, Arnold AP, Berkley KJ, Blaustein JD, Eckel LA, Hampson E, Herman JP, Marts S, Sadee W, Steiner M, Taylor J, Young E. Strategies and methods for research on sex differences in brain and behavior. Endocrinology 2005;146:1650–1673. [PubMed: 15618360]
7. Berkley KJ, Dmitrieva N, Curtis KS, Papka RE. Innervation of ectopic endometrium in a rat model of endometriosis. Proc Natl Acad Sci USA 2004;101:11094–11098. [PubMed: 15256593]

8. Berkley KJ, Rapkin AJ, Papka RE. The pains of endometriosis. Science 2005;308:1587–1589. [PubMed: 15947176]
9. Birder LA, Perl ER. Expression of alpha2-adrenergic receptors in rat primary afferent neurones after peripheral nerve injury or inflammation. J Physiol 1999;515:533–542. [PubMed: 10050019]
10. Bjorling DE, Wang ZY. Estrogen and neuroinflammation. Urology 2001;57:40–46. [PubMed: 11378049]
11. Bolay H, Moskowitz MA. The emerging importance of cortical spreading depression in migraine headache. Rev Neurol (Paris) 2005;161:655–657. [PubMed: 16141950]
12. Bourley V, Volkov N, Pavlovitch S, Lets N, Larsson A, Ovsson M. The relationship between microvessel density, proliferative activity and expression of vascular endothelial growth factor-A and its receptors in eutopic endometrium and endometriotic lesions. Reproduction 2006;132:501–509. [PubMed: 16940291]
13. Carmeliet P. Angiogenesis in life, disease and medicine. Nature 2005;438:932–936. [PubMed: 16355210]
14. Carmeliet P, Tessier-Lavigne M. Common mechanisms of nerve and blood vessel wiring. Nature 2005;436:193–200. [PubMed: 16015319]
15. Cason AM, Samuelsen CL, Berkley KJ. Estrous changes in vaginal nociception in a rat model of endometriosis. Horm Behav 2003;44:123–131. [PubMed: 13129484]
16. Chabal C, Jacobson L, Russell LC, Burchiel KJ. Pain response to perineuromal injection of normal saline, epinephrine, and lidocaine in humans. Pain 1992;49:9–12. [PubMed: 1594285]
17. Chung K, Lee BH, Yoon YW, Chung JM. Sympathetic sprouting in the dorsal root ganglia of the injured peripheral nerve in a rat neuropathic pain model. J Comp Neurol 1996;376:241–252. [PubMed: 8951640]
18. Clatworthy AL, Illich PA, Castro GA, Walters ET. Role of peri-axonal inflammation in the development of thermal hyperalgesia and guarding behavior in a rat model of neuropathic pain. Neurosci Lett 1995;184:5–8. [PubMed: 7739805]
19. Deng YS, Zhong JH, Zhou XF. Effects of endogenous neurotrophins on sympathetic sprouting in the dorsal root ganglia and allodynia following spinal nerve injury. Exp Neurol 2000;164:344–350. [PubMed: 10915573]
20. Drummond PD. Noradrenaline increases hyperalgesia to heat in skin sensitized by capsaicin. Pain 1995;60:311–315. [PubMed: 7596627]
21. Evans S, Moalem-Taylor G, Tracey DJ. Pain and endometriosis. Pain 2007;132:S22–S25. [PubMed: 17761388]
22. Fasciani A, D'Ambrogio G, Bocci G, Monti M, Genazzani AR, Artini PG. High concentrations of the vascular endothelial growth factor and interleukin-8 in ovarian endometriomata. Mol Hum Reprod 2000;6:50–54. [PubMed: 10611260]
23. Ferrara N. Vascular endothelial growth factor: basic science and clinical progress. Endocr Rev 2004;25:581–611. [PubMed: 15294883]
24. Ferriani RA, Charnock-Jones DS, Prentice A, Thomas EJ, Smith SK. Immunohistochemical localization of acidic and basic fibroblast growth factors in normal human endometrium and endometriosis and the detection of their mRNA by polymerase chain reaction. Hum Reprod 1993;8:11–16. [PubMed: 7681435]
25. Freemont AJ, Watkins A, Le MC, Baird P, Jeziorska M, Knight MT, Ross ER, O'Brien JP, Hoyland JA. Nerve growth factor expression and innervation of the painful intervertebral disc. J Pathol 2002;197:286–292. [PubMed: 12115873]
26. Fujimoto J, Sakaguchi H, Hirose R, Tamaya T. Expression of platelet-derived endothelial cell growth factor (PD-ECGF) related to angiogenesis in ovarian endometriosis. J Clin Endocrinol Metab 1999;84:359–362. [PubMed: 9920107]
27. Gazvani R, Templeton A. Peritoneal environment, cytokines and angiogenesis in the pathophysiology of endometriosis. Reproduction 2002;123:217–226. [PubMed: 11866688]
28. Giudice LC, Kao LC. Endometriosis. Lancet 2004;364:1789–1799. [PubMed: 15541453]
29. Grelik C, Bennett GJ, Ribeiro-da-Silva A. Autonomic fibre sprouting and changes in nociceptive sensory innervation in the rat lower lip skin following chronic constriction injury. Eur J Neurosci 2005;21:2475–2487. [PubMed: 15932605]

30. Groothuis PG, Nap AW, Winterhager E, Grummer R. Vascular development in endometriosis. Angiogenesis 2005;8:147–156. [PubMed: 16211360]
31. Hamel E. Perivascular nerves and the regulation of cerebrovascular tone. J Appl Physiol 2006;100:1059–1064. [PubMed: 16467392]
32. Harada T, Iwabe T, Terakawa N. Role of cytokines in endometriosis. Fertil Steril 2001;76:1–10. [PubMed: 11438312]
33. Hill RG, Oliver KR. Neuropeptide and kinin antagonists. Handb Exp Pharmacol 2007:181–216. [PubMed: 17087124]
34. Hull ML, Charnock-Jones DS, Chan CL, Bruner-Tran KL, Osteen KG, Tom BD, Fan TP, Smith SK. Antiangiogenic agents are effective inhibitors of endometriosis. J Clin Endocrinol Metab 2003;88:2889–2899. [PubMed: 12788903]
35. Hyder SM. Sex-steroid regulation of vascular endothelial growth factor in breast cancer. Endocrinol Relat Cancer 2006;13:667–687.
36. Jones MG, Munson JB, Thompson SW. A role for nerve growth factor in sympathetic sprouting in rat dorsal root ganglia. Pain 1999;79:21–29. [PubMed: 9928772]
37. Kaplan DR, Miller FD. Signal transduction by the neurotrophin receptors. Curr Opin Cell Biol 1997;9:213–221. [PubMed: 9069267]
38. Lazarovici P, Marcinkiewicz C, Lelkes PI. Cross talk between the cardiovascular and nervous systems: neurotrophic effects of vascular endothelial growth factor (VEGF) and angiogenic effects of nerve growth factor (NGF)-implications in drug development. Curr Pharm Des 2006;12:2609–2622. [PubMed: 16842161]
39. Lowe EM, Anand P, Terenghi G, Williams-Chestnut RE, Sinicropi DV, Osborne JL. Increased nerve growth factor levels in the urinary bladder of women with idiopathic sensory urgency and interstitial cystitis. Br J Urol 1997;79:572–577. [PubMed: 9126085]
40. Luts L, Sundler F. Autotransplantation of rat parathyroid glands: a study on morphological changes. Transplantation 1998;66:446–453. [PubMed: 9734486]
41. McLachlan EM, Janig W, Devor M, Michaelis M. Peripheral nerve injury triggers noradrenergic sprouting within dorsal root ganglia. Nature 1993;363:543–546. [PubMed: 8505981]
42. McLaren J, Prentice A, Charnock-Jones DS, Smith SK. Vascular endothelial growth factor (VEGF) concentrations are elevated in peritoneal fluid of women with endometriosis. Hum Reprod 1996;11:220–223. [PubMed: 8671190]
43. Michaelis M, Devor M, Janig W. Sympathetic modulation of activity in rat dorsal root ganglion neurons changes over time following peripheral nerve injury. J Neurophysiol 1996;76:753–763. [PubMed: 8871196]
44. Miller LJ, Fischer KA, Goralnick SJ, Litt M, Burleson JA, Albertsen P, Kreutzer DL. Nerve growth factor and chronic prostatitis/chronic pelvic pain syndrome. Urology 2002;59:603–608. [PubMed: 11927336]
45. Mueller MD, Vigne JL, Minchenko A, Lebovic DI, Leitman DC, Taylor RN. Regulation of vascular endothelial growth factor (VEGF) gene transcription by estrogen receptors alpha and beta. Proc Natl Acad Sci USA 2000;97:10972–10977. [PubMed: 10995484]
46. Nagabukuro H, Berkley KJ. Influence of endometriosis on visceromotor and cardiovascular responses induced by vaginal distention in the rat. Pain. 2007 May 31;Epub ahead of print
47. Papka RE. Some nerve endings in the rat pelvic paracervical autonomic ganglia and varicosities in the uterus contain calcitonin gene-related peptide and originate from dorsal root ganglia. Neuroscience 1990;39:459–470. [PubMed: 2128374]
48. Papka, RE.; Traurig, HH. Autonomic efferent and visceral sensory innervation of the female reproductive system: special reference to neurochemical markers in nerves and ganglionic connections. In: Maggi, CA., editor. Nervous Control of the Urogenital System. New York: Harwood; 1993. p. 421-464.
49. Papka RE, McNeill DL, Thompson D, Schmidt HH. Nitric oxide nerves in the uterus are parasympathetic, sensory, and contain neuropeptides. Cell Tissue Res 1995;279:339–349. [PubMed: 7534654]
50. Pezet S, McMahon SB. Neurotrophins: mediators and modulators of pain. Annu Rev Neurosci 2006;29:507–538. [PubMed: 16776595]

51. Punnonen J, Teisala K, Ranta H, Bennett B, Punnonen R. Increased levels of interleukin-6 and interleukin-10 in the peritoneal fluid of patients with endometriosis. Am J Obstet Gynecol 1996;174:1522–1526. [PubMed: 9065123]
52. Ramer MS, Bisby MA. Rapid sprouting of sympathetic axons in dorsal root ganglia of rats with a chronic constriction injury. Pain 1997;70:237–244. [PubMed: 9150299]
53. Reimer MK, Mokshagundam SP, Wyler K, Sundler F, Ahren B, Stagner JI. Local growth factors are beneficial for the autonomic reinnervation of transplanted islets in rats. Pancreas 2003;26:392–397. [PubMed: 12717274]
54. Rogers PA, Gannon BJ. The vascular and microvascular anatomy of the rat uterus during the oestrous cycle. Aust J Exp Biol Med Sci 1981;59:667–679. [PubMed: 7200355]
55. Roush W. Receptor links blood vessels, axons. Science 1998;279:2042. [PubMed: 9537914]
56. Rueff A, Mendell LM. Nerve growth factor NT-5 induce increased thermal sensitivity of cutaneous nociceptors in vitro. J Neurophysiol 1996;76:3593–3596. [PubMed: 8930301]
57. Ruocco I, Cuello AC, Ribeiro-da-Silva A. Peripheral nerve injury leads to the establishment of a novel pattern of sympathetic fibre innervation in the rat skin. J Comp Neurol 2000;422:287–296. [PubMed: 10842232]
58. Sharpe-Timms KL. Endometrial anomalies in women with endometriosis. Ann NY Acad Sci 2001;943:131–147. [PubMed: 11594534]
59. Sharpe-Timms KL. Using rats as a research model for the study of endometriosis. Ann NY Acad Sci 2002;955:318–327. [PubMed: 11949958]
60. Shi Z, Arai KY, Jin W, Weng Q, Watanabe G, Suzuki AK, Taya K. Expression of nerve growth factor and its receptors NTRK1 and TNFRSF1B is regulated by estrogen and progesterone in the uteri of golden hamsters. Biol Reprod 2006;74:850–856. [PubMed: 16436532]
61. Shifren JL, Tseng JF, Zaloudek CJ, Ryan IP, Meng YG, Ferrara N, Jaffe RB, Taylor RN. Ovarian steroid regulation of vascular endothelial growth factor in the human endometrium: implications for angiogenesis during the menstrual cycle and in the pathogenesis of endometriosis. J Clin Endocrinol Metab 1996;81:3112–3118. [PubMed: 8768883]
62. Sofroniew MV, Howe CL, Mobley WC. Nerve growth factor signaling, neuroprotection, and neural repair. Annu Rev Neurosci 2001;24:1217–1281. [PubMed: 11520933]
63. Sondell M, Sundler F, Kanje M. Vascular endothelial growth factor is a neurotrophic factor which stimulates axonal outgrowth through the flk-1 receptor. Eur J Neurosci 2000;12:4243–4254. [PubMed: 11122336]
64. Suchting S, Bicknell R, Eichmann A. Neuronal clues to vascular guidance. Exp Cell Res 2006;312:668–675. [PubMed: 16330027]
65. Taketani Y, Kuo TM, Mizuno M. Comparison of cytokine levels and embryo toxicity in peritoneal fluid in infertile women with untreated or treated endometriosis. Am J Obstet Gynecol 1992;167:265–270. [PubMed: 1442940]
66. Vercellini P. Endometriosis: what a pain it is. Semin Reprod Endocrinol 1997;15:251–61. [PubMed: 9383834]
67. Vernon MW, Wilson EA. Studies on the surgical induction of endometriosis in the rat. Fertil Steril 1985;44:684–694. [PubMed: 4054348]
68. Watkins LR, Maier SF, Goehler LE. Immune activation: the role of pro-inflammatory cytokines in inflammation, illness responses and pathological pain states. Pain 1995;63:289–302. [PubMed: 8719529]
69. Weihe E, Schafer MK, Erickson JD, Eiden LE. Localization of vesicular monoamine transporter isoforms (VMAT1 and VMAT2) to endocrine cells and neurons in rat. J Mol Neurosci 1994;5:149–164. [PubMed: 7654518]
70. Woolf CJ, Allchorne A, Safieh-Garabedian B, Poole S. Cytokines, nerve growth factor and inflammatory hyperalgesia: the contribution of tumour necrosis factor alpha. Br J Pharmacol 1997;121:417–424. [PubMed: 9179382]
71. Yen LD, Bennett GJ, Ribeiro-da-Silva A. Sympathetic sprouting and changes in nociceptive sensory innervation in the glabrous skin of the rat hind paw following partial peripheral nerve injury. J Comp Neurol 2006;495:679–690. [PubMed: 16506190]

72. Zoubina EV, Fan Q, Smith PG. Variations in uterine innervation during the estrous cycle in rat. J Comp Neurol 1998;397:561–571. [PubMed: 9699916]

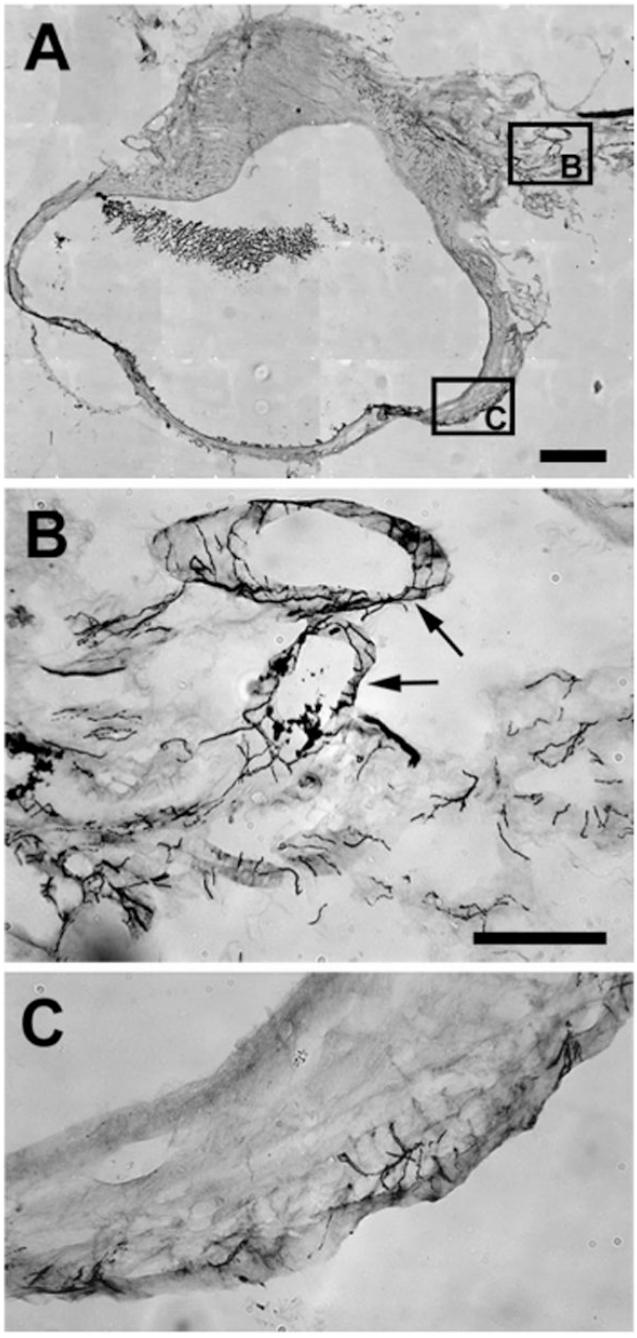

Fig. 1.

Photomicrographs of parts of a section immunostained with vesicular monoamine transporter (VMAT). *A*: Low-power view of area where photomicrographs in B and C were taken. *B*: at the entrance to the cyst, neurites are very dense and associated mainly with blood vessels (arrows) as they enter the wall of the cyst in the hilus region. *C*: further into the cyst, these neurites become less dense but also extend into the myometrium and epithelial lining. Note that this pattern was the same for neurites stained with other markers and for the uterine horn. Calibration bar: 500 μm for *A*; 100 μm for *B* and *C*.

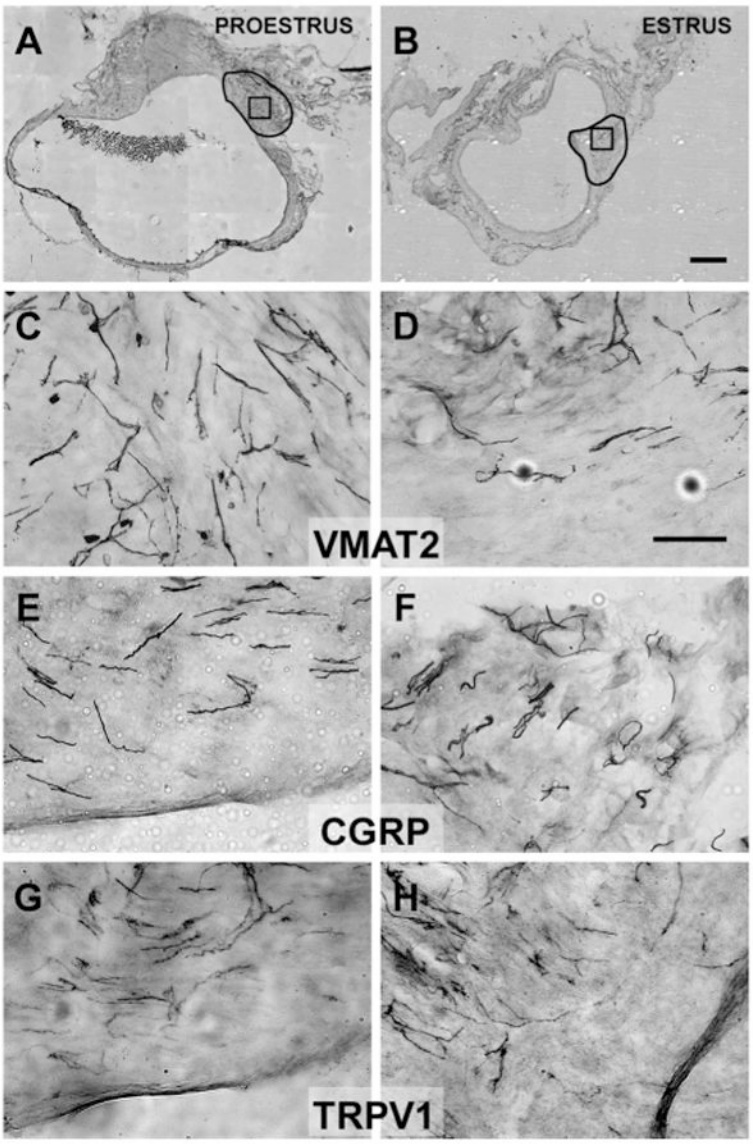

Fig. 2.

The regions outlined in *A* and *B* indicate the hilus region of two cysts, within which neurite labeling was counted (see *Immunohistochemistry* section in METHODS). The boxes in *A* and *B* (within the outline) indicate the approximate region where the higher-power photomicrographs (*C–H*) were taken. Photomicrographs of sections immunostained with antibodies for VMAT2 (*C* and *D*), CGRP (*E* and *F*), or transient receptor potential vanilloid-1 (TRPV1) (*G* and *H*) in the wall of cysts in proestrus (*left*) or estrus (*right*). Note that the density of neurites positively immunostained by VMAT2 (sympathetic fibers) was greater in proestrus than estrus, whereas there were no proestrous-to-estrous differences in the density of neurites positively immunostained by CGRP and TRPV1 (sensory fibers). Calibration bar: 500 μm for *A* and *B*; 50 μm for *C–H*.

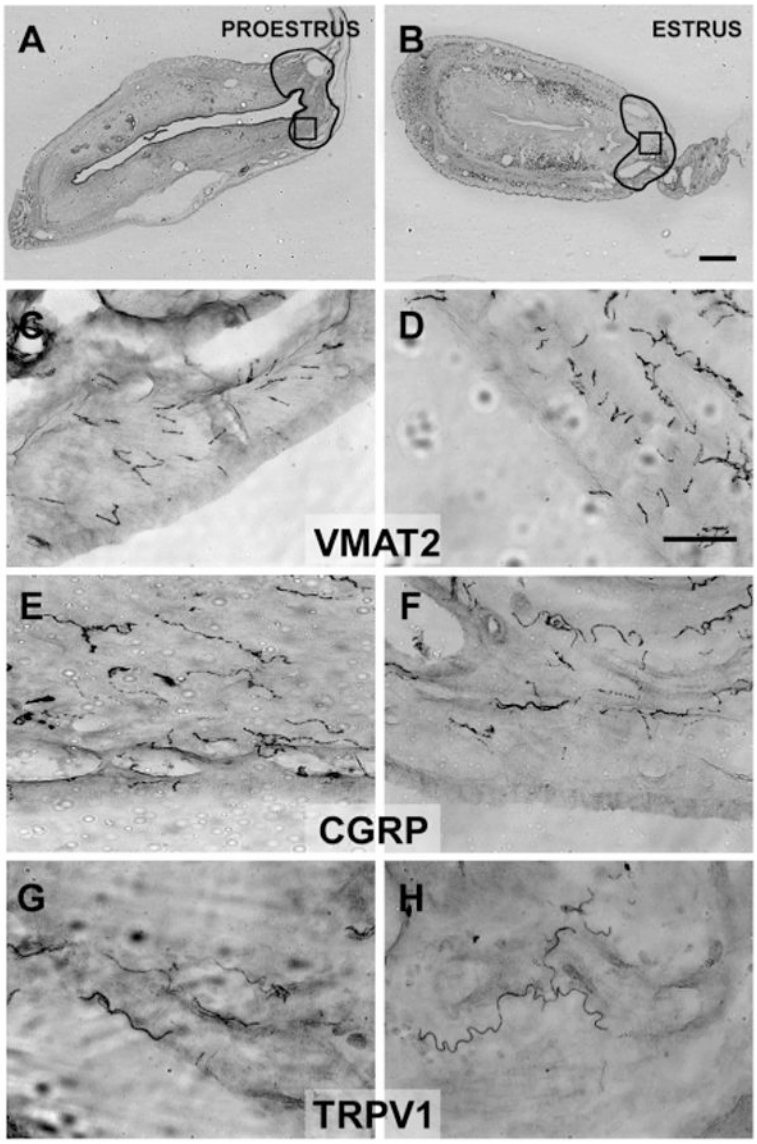

Fig. 3.

The regions outlined in *A* and *B* indicate an area in the uterine horn comparable to the hilus in the cysts (see Fig. 2, A and B), within which neurite labeling was counted (see *Immunohistochemistry* section in METHODS). The boxes in *A* and *B* (within the outlines) indicate the approximate regions where the higher-power photomicrographs (*C–H*) were taken. Photomicrographs of sections immunostained with antibodies for VMAT2 (*C* and *D*), CGRP (*E* and *F*), and TRPV1 (*G* and *H*) in the wall of the uterine horn in proestrus (*left*) or estrus (*right*). There were no proestrous-to-estrous differences in the density of neurite labeling for any of the markers. Calibration bar: 500 μm for *A* and *B*; 50 μm for *C–H*.

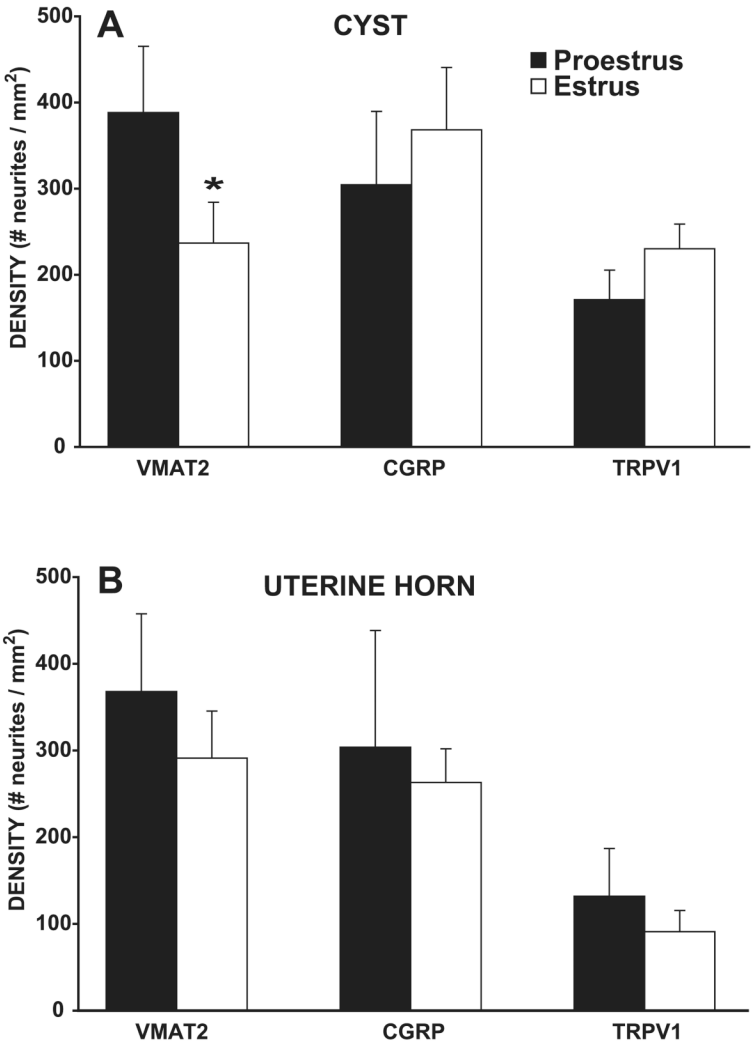

Fig. 4.

Density of neurites in the hilus region of the cysts (*A*) and uterine horn (*B*) immunostained with VMAT2, CGRP, and TRPV1 ~11 wk after endometriosis (ENDO) surgery. In the cysts, the density of sympathetic fibers labeled by VMAT2 was significantly greater in proestrus than estrus, whereas the density of neurites labeled with the other markers showed no significant proestrous-to-estrous differences. In proestrus (but not estrus), the density of TRPV1 neurites was less than the density of sympathetic neurites. In the uterine horn, there were no proestrous-to-estrous differences in the density of neurites labeled by any of the markers. In both stages, the density of TRPV1 neurites was signficantly less than the density of sympathetic and CGRP labeled neurites. Data are shown as means ± SE. **P* < 0.05 compared with proestrus.

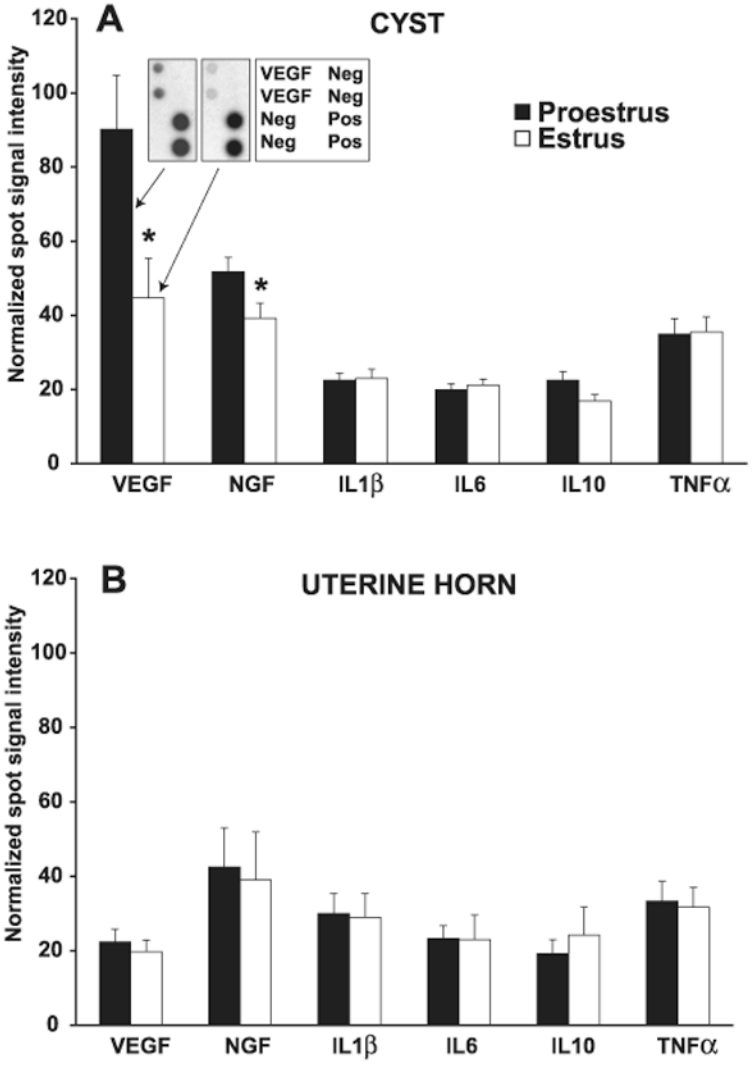

Fig. 5.

Normalized spot signal intensities on films of protein array membranes of growth factors and cytokines in the cysts (*A*) and in the uterine horn (*B*) in proestrus or estrus ~11 wk after ENDO surgery. In the cysts, the levels of growth factors VEGF and NGF, but not the cytokines, including IL-1β, IL-6, IL-10, and TNF-α, were significantly higher in proestrus than estrus. In contrast, there were no proestrus-to-estrus differences in the levels of any of these six proteins in the uterine horn. VEGF levels were greater in the cysts than in the uterine horn in proestrus but not estrus. There were no differences in cyst-uterine horn levels for the other proteins. Data are shown as means ± SE. **P* < 0.05, compared with proestrus. *A*, *inset*: examples of a portion of developed films from two arrays showing double spots for the VEGF antibody, and the positive (Pos) and negative (Neg) controls. One film was from an array of a cyst in proestrus (*left* spots) and the other was from an array of another cyst in estrus (*right* spots). A key for the two arrays is shown in the table next to them.

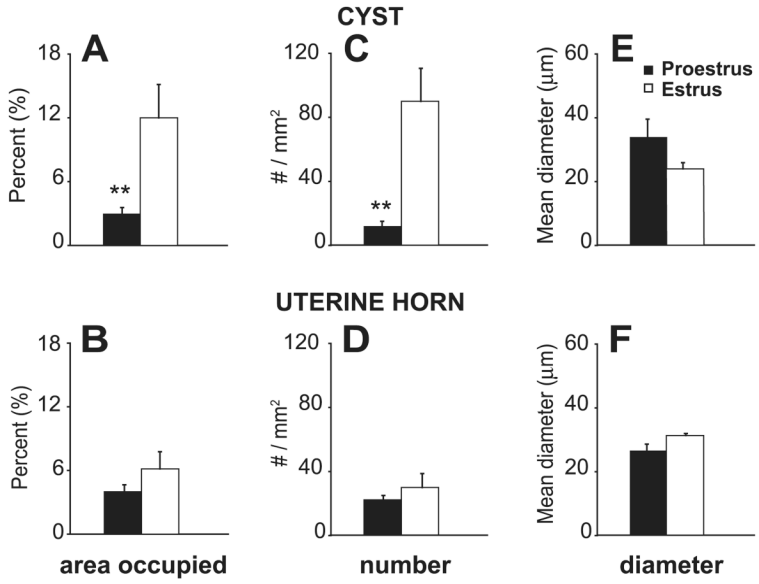

Fig. 6.

Vascularization of the cysts and uterine horn in proestrus and estrus. *A* and *B*: percentage of the total area occupied by blood vessels (BV) in the cysts and uterine horn, respectively. *C* and *D*: number of BVs within that area of the cysts and uterine horn, respectively. *E* and *F*: mean diameter of BVs in that area of the cysts and uterine horn, respectively. Note that there were significant proestrous-to-estrous changes in vascularization of the cysts but not the uterine horn. In the cysts, from proestrus-to-estrus, there was a small insignificant decrease in the diameter of BVs (*E*) and a large, significant increase in the number of BVs (*C*), resulting in an overall significant increase in the percentage of the total area occupied by BVs (*A*). In contrast, there were no significant estrous changes in vascularization of the uterine horn. Data are shown as means ± SE. $^{**}P < 0.01$, compared with estrus.

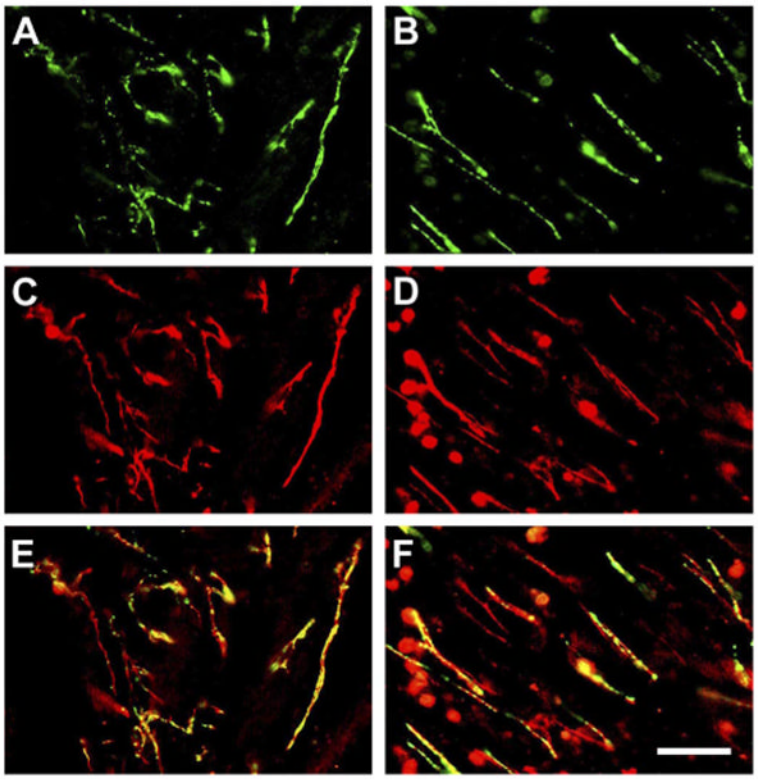

Fig. 7.

Examples showing photomicrographs of sections of cysts double-immunostained with TrkA and VMAT2, or TrkA and CGRP antibodies. Green indicates single labeling for VMAT2 (*A*) or CGRP (*B*). Red indicates single labeling for TrkA (*C* and *D*). Yellow and/or orange indicates double labeling of TrKA with VMAT2 (*E*) or TrkA with CGRP (*F*). Calibration bar, 50 μm for *A*–*F*.